Journal of Ceramic Processing Research. Vol. 17, No. 12, pp. 1279~1282 (2016)

J O U R N A L O F
Ceramic Processing Research

Effect of flow rate of atmosphere gases on the characteristics of Mo-doped ZnO (MZO) thin films

Yeong-Jin Lee, Yong-Ho Lee, Ji-Hoon Jeong and Kyu-Mann Lee*
Korea University of Technology and Education, 307, Gajeon-ri, Byungcheon-myun, Cheonan-city, Chungnam 330-708, Korea

We have investigated the effect of ambient gases on the characteristics of Mo-doped ZnO (MZO) thin films. The MZO thin films are deposited by radio frequency (RF) magnetron sputtering under different ambient gases (Ar, Ar+O_2, and Ar+H_2) at 100 °C. To investigate the influences of the ambient gases, the flow rate of oxygen and hydrogen in argon was varied from 0.1 sccm to 0.5 sccm. The MZO thin films were preferentially oriented to the (002) direction, regardless of the ambient gases used. The electrical resistivity of the MZO thin films increased with increasing O_2 flow rates, whereas the electrical resistivity decreased sharply under an Ar+H_2 atmosphere and was nearly the same, regardless of the H_2 flow rate used. The change of electrical resistivity with changes in the ambient gas composition was mainly interpreted in terms of the charge carrier concentration rather than the charge carrier mobility. All the films showed an average transmittance of over 80% in the visible range. The optical band gap of the MZO films increased with increasing H_2 flow rates, whereas the optical band gap of the MZO films deposited under an O_2 atmosphere slightly decreased with increasing O_2 flow rates.

Key words: MZO thin film, ambient gas, RF sputtering, Optical band gap.

Introduction

Transparent conducting oxide (TCO) thin films have been extensively studied, especially for their applications to display devices such as LCDs and OLEDs [1-3]. Of all the TCO thin films, indium tin oxide (ITO) thin films have been extensively utilized in these devices because of their high transmittance in the visible range and low electrical resistivity [4, 5]. However, indium is a relatively scarce element in the earth's crust, leading to high costs for ITO production. The other drawback of ITO thin films is the unstable nature of the film in a reduced ambient atmosphere. The indium from the ITO layer can diffuse into the organic materials, which leads to significant deterioration of the device reliability [4, 5].

Recently, new transparent conducting oxide such as MZO (Mo-doped zinc oxide) thin films have emerged as promising anode materials for OLEDs due to low resistivity, excellent thermal stability, and high transmittance over 85% in the visible spectrum range [6-12]. The properties of MZO thin films strongly depend on the stoichiometry, microstructure, and the nature of the impurities, and therefore, it is obvious that deposition processes associated with different processing control parameters induce slightly different characteristics in MZO thin films [6-12]. The effect of oxygen and hydrogen in the reactive sputtering process on the structural, electrical and optical properties of TCO films has been studied by several groups [13-19]. From these studies, it is concluded that the electrical resistivity and the optical property strongly correlates with the stoichiometry of the MZO thin films. Considering these facts, it is interesting to study the effect of the ambient gas on the structure, the electrical resistivity, and the optical band gap energy of the MZO thin films. For this purpose, MZO thin films were deposited by RF magnetron sputtering under various ambient gases (Ar, Ar+O_2, and Ar+H_2). The electrical resistivity and the optical band gap of the MZO thin films were systematically examined.

*Corresponding author:
Tel : +82-41-560-1320
Fax: +82-41-560-1360
E-mail: kmlee@koreatech.ac.kr

Experimental

The MZO thin films were prepared by RF magnetron sputtering with a mixture of a 98% zinc oxide and 2% mol molybdenum oxide target. The glass substrates (Corning 7059) were first cleaned with standard cleaning procedures and then rinsed in deionized water. The sputtering chamber was evacuated by a turbomolecular pump to a base pressure of approximately 6.0×10^{-6} torr. To investigate the influences of the oxygen and hydrogen, the flow rate of oxygen and hydrogen in the argon mixing gas has been varied from 0.1 sccm to 0.5 sccm. The sputtering gas was Ar and the substrate temperature was 100 °C. Table 1 indicates the experimental conditions for the deposition of MZO thin films.

The microstructure, surface characteristics, and crystal orientation of the MZO thin films were evaluated by using a field emission scanning electron microscope (Jeol, JSM7500F), AFM (Pucotech, MOD-1 M), and X-ray diffraction (Rigaku, RTP300RC), respectively. The

Table 1. Sputtering conditions of MZO thin films.

Deposition parameters	Conditions
Target	MoO_3/ZnO(2/98 wt.%)
Target diameter (inch)	3
Substrate	Glass (Corning 7059)
Working pressure (Pa)	6.67×10^{-1}
Film thickness (nm)	200
Substrate temperature (°C)	100
RF power (W)	100
Gas ambient (sccm)	Ar:40, O_2 flow rate:0.1-0.5, H_2 flow rate:0.1-0.5

optical transmittance of MZO thin films was measured using an ultraviolet spectrophotometer (model Cary 500, Varian, KOR). The electrical properties of the MZO thin films were measured using Hall effect measurements (model HMS-3000, Ecopia, KOR).

Results and Discussion

XRD patterns of the MZO thin films deposited using RF magnetron sputtering are presented in Fig. 1. The figure clearly indicates that the MZO phase is fully stabilized (within the detection limit of XRD), and the (002) peak is the most prominent peak, indicating that the MZO film has a (001) preferential orientation. Furthermore, with the increase in the oxygen and hydrogen concentrations, the intensity of the (002) peak remains unchanged. It has been reported that sputtered ZnO thin films are polycrystalline with a c-axis preferred orientation, which is mainly due to the low surface energy of the (0001) plane in ZnO [13]. Based on the above discussion, we can conclude that the (001) plane of MZO thin films has the lowest surface energy.

Microstructural features of the MZO thin films with different ambient gases are presented in Fig. 2. As shown in the figures, the second phases are not observed. The grain sizes in MZO thin films deposited under Ar+O_2 and Ar+H_2 ambient gases are nearly the same, regardless of the ambient gas flow rate. From the results of Figs. 1 and 2, it seems that the ambient gases have an important effect upon the physical characteristics, such as the crystal orientation and the microstructure of the thin films.

Because the surface properties of the TCO thin films may affect the characteristics of the OLED devices [20], it is very important to investigate the surface morphology of the TCO thin films. Figure 3 presents the AFM images of MZO thin films deposited under the various ambient gases. As shown in the figures, all surfaces are very flat, and no sharp peaks appear in the domain. Furthermore, it seems that the surface roughness is not directly related to the concentration and type of ambient gas.

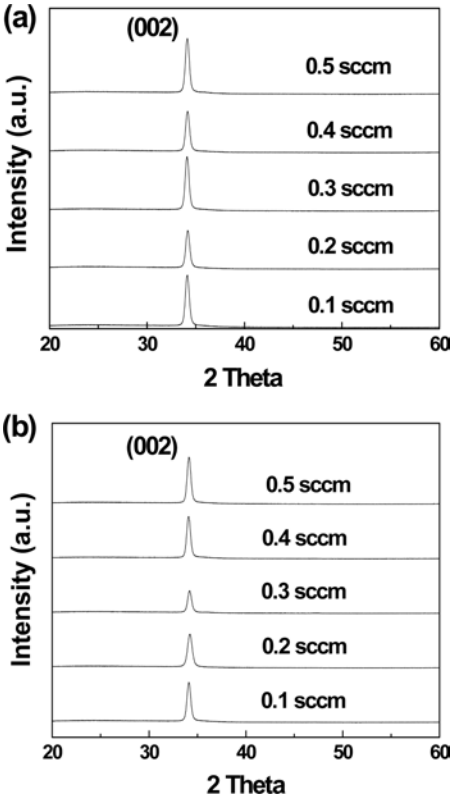

Fig. 1. XRD patterns of MZO thin films deposited under (a) O_2 and (b) H_2 with Ar gas.

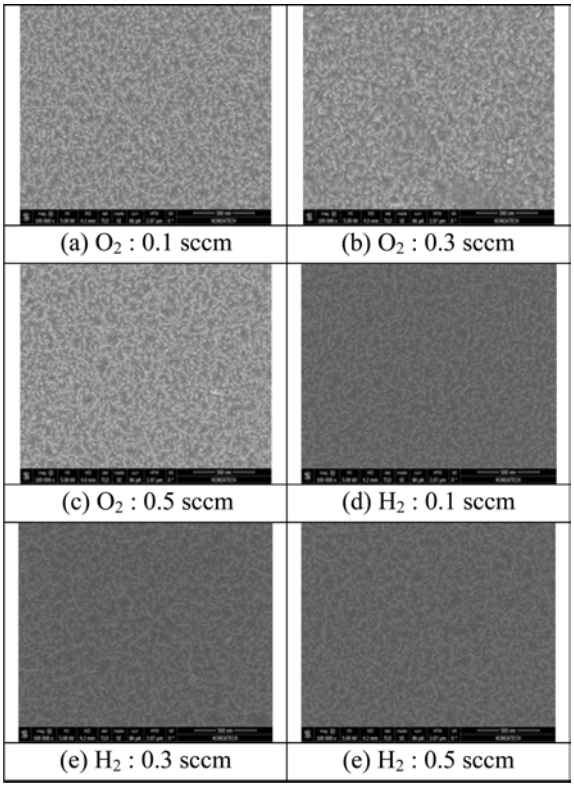

Fig. 2. FESEM images of MZO thin films with different ambient gases.[1]

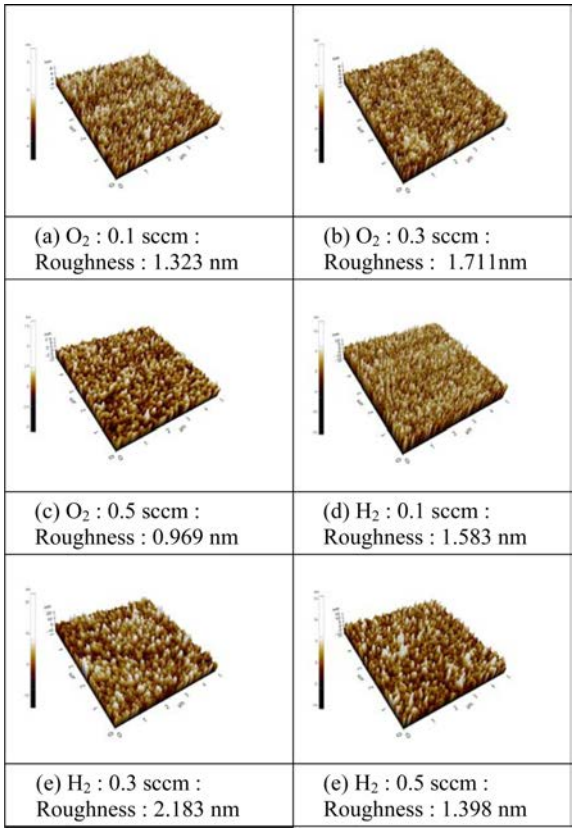

Fig. 3. AFM morphologies of the MZO films deposited with different ambient gases.

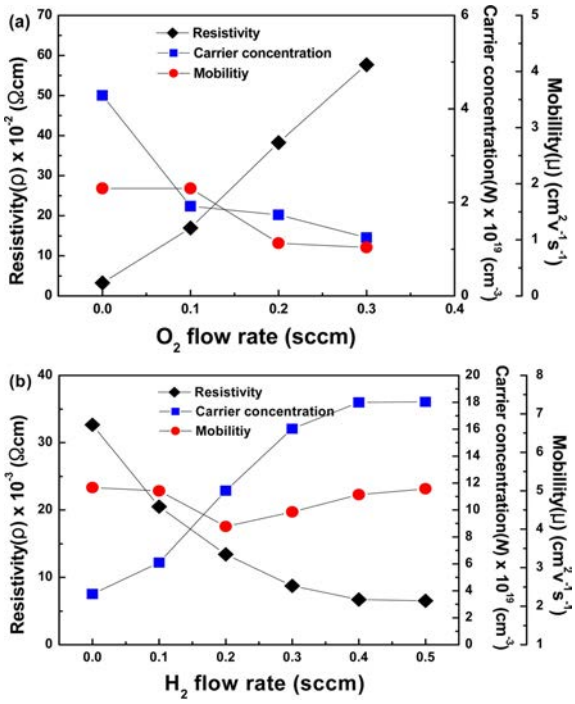

Fig. 4. Resistivity (ρ), mobility (μ) and carrier concentration (*N*) of MZO thin films with flow rate of (a) O_2 and (b) H_2 with Ar.

Figure 4 presents the electrical resistivity (ρ), charge mobility (μ), and charge carrier concentration (*N*) of

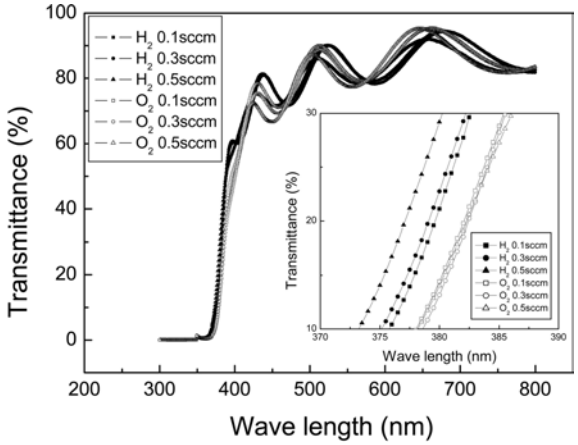

Fig. 5. Optical transmittance spectra of MZO films deposited under different ambient gases (Ar, Ar+O_2, and Ar+H_2).

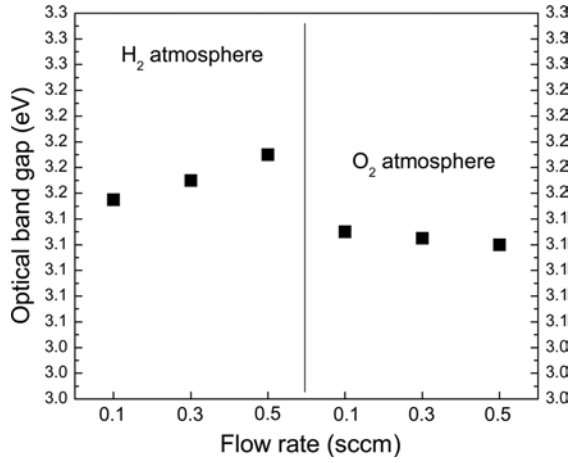

Fig. 6. Optical band gap of MZO thin films as a function of the flow rate of O_2 and H_2 with Ar.

the MZO thin films with flow rates of (a) O_2 and (b) H_2. As shown in the figures, the resistivity of the MZO films increases with increasing O_2 flow rate, which can be interpreted in terms of the decrease in the charge carrier concentration. The electrical resistivity decreases very sharply under an Ar+H_2 atmosphere and is nearly the same, regardless of the H_2 flow rate. This can be interpreted in terms of the drastic increase in the the charge carrier concentration. From the results of Fig. 4, it is important to note that the electrical resistivity of MZO thin films is mainly associated with the charge carrier concentration rather than the charge carrier mobility. It is now well established that oxygen vacancies in ZnO based TCO thin films act as donors, and their presence make the film less resistive [21]. During reactive sputtering under ambient oxygen the thin film becomes more stoichiometric, and the concentration of oxygen vacancies decreases. Thus, the electrical resistivity increases. Under reactive sputtering with hydrogen, due to the reducing property of hydrogen, oxygen vacancies are created in MZO thin films. Therefore, the resistivity of such films deposited under an Ar+H_2 ambient

environment is much lower than the resistivity of films deposited under $Ar+O_2$.

Figure 5 presents the optical property of the MZO thin films with different ambient gases. The figure shows that the average transmittance in the visible wavelength region is over 80% for all the MZO thin films. As clearly seen in the inset of Fig. 5, the UV absorption edge shifted by a small wavelength with decreasing O_2 flow rates and increasing H_2 flow rates, indicating broadening of the optical band gap.

We can assume that the absorption coefficient $\alpha = (1/d)\ln(1/T)$, where T is the transmittance and d is the thin film thickness (200 nm in our experiment). The optical band gap energy (E_{opt}) of the MZO thin films can be determined from the experimental spectra of the absorption coefficient (α) as a function of the photon energy ($h\upsilon$) using the following equation [22]:

$$(\alpha h\upsilon)^2 = C(h\upsilon - E_{opt}) \quad (1)$$

where C is a constant for a direct transition, h is Planck's constant, and υ is the frequency of the incident photon.

The optical band gap energies (E_{opt}) of the MZO films are shown in Fig. 6. As shown in the figure, the optical band gap of the MZO films increases with increasing H_2 flow rates. However, it seems that the optical band gap of the MZO films deposited under an O_2 atmosphere slightly decreases with increasing O_2 flow rates. It has been reported that an increase in the Fermi level in the conduction band of degenerate semiconductors leads to a band gap widening effect, which is consistent with our experimental results [18, 19, 23].

Conclusions

The effect of ambient gases on the characteristics such as structural, electrical, and optical properties of Mo-doped ZnO (MZO) thin was systematically examined. MZO thin films were deposited by RF magnetron sputtering under different ambient gas combinations (Ar, $Ar+O_2$, and $Ar+H_2$). All the MZO thin films had an (002) preferential orientation, regardless of the ambient gases used. The electrical resistivity of the MZO thin films increased with increasing O_2 flow rates, and dramatically decreased under an $Ar+H_2$ atmosphere. The electrical resistivity of MZO thin films was mainly associated with the charge carrier concentration. All the MZO thin films had a high transmittance, regardless of the ambient gases used. The optical band gap of the MZO films increased with increasing H_2 flow rates and slightly decreased with increasing O_2 flow rates.

References

1. K. Tominaga, T. Ueda, T. Ao, M. Kataoka, and I. Mori, Thin Solid Films 281-282 (1996) 194-197.
2. Y. Hoshi, H. Kato, and K. Funatsu, Thin Solid Films 445 (2003) 245-250.
3. K. Ishibashi, K. Hirata, and N. Hosokawa, Journal of Vacuum Science & Technology A 10 (1992) 1718-1722.
4. N. Taga, M. Maekawa, Y. Shigesato, I. Yasui, M. Kamei, and T.E. Haynes, Jpn. J. Appl. Phys. 37 (1998) 6524-6529.
5. C. Nunes de Carvalho, A. M. Botelho do Rego, A. Amaral, P. Brogueira, and G. Lavareda, Surface and Coatings Technology 124 (2000) 70-75.
6. X. Xiu, Z. Pang, M. Lv, Y. Dai, L. Ye, and S. Han, Appl. Surf. Sci. 253 (2007) 3345-3348.
7. X. Xiu, Y. Cao, Z. Pang, M. Lv, and S. Han, J. Mater. Sci. Technol. 25 (2009) 785-788.
8. Y.C. Lin, B.L. Wang, W.T. Yen, C.T. Ha, and C. Peng, Thin Solid Films 518 (2010) 4928-4934.
9. X.X. Xu and Z.W. Jing, Chin. Phys. B 21 (2012) 066802.
10. I. Soumahoro, S. Colis, G. Schmerber, C. Leuvrey, S. Barre, C. Ulhaq-Bouillet, D. Muller, M. Abd-lefdil, N. Hassanain, J. Petersen, A. Berrada, A. Slaoui, and A. Dinia, Thin Solid Films 566 (2014) 61-69.
11. J.W. Zhang, G. He, T.S. Li, M. Liu, X.S. Chen, Y.M. Liu, and Z.Q. Sun, Mater. Res. Bull. 65 (2015) 7-13.
12. M. Wu, S. Yu, G. Chen, L. He, L. Yang, and W. Zhang, Appl. Surf. Sci. 324 (2015) 791-796.
13. K.H. Yoon, J.W. Choi, and D.H. Lee, Thin Solid Films 302 (1997) 116-121.
14. W. Liu, G. Du, Y. Sun, Y. Xu, T. Yang, X. Wang, Y. Chang, and F. Qiu, Thin Solid Flms 515 (2007) 3057-3060.
15. X. Hou, K.L. Choy, and J.P. Liu, J. Nanosci. Nanotechnol. 11 (2011) 8114-8119.
16. J.H. Bang, H.W. Park, S.H. Cho, and P.K. Song, J. Nanosci. Nanotechnol. 12 (2012) 3425-3429.
17. N. Oka, K. Kimura, T. Yagi, N. Taketoshi, T. Baba, and Y. Shigesato, J. Appl. Phys. 111 (2112) 093701.
18. Y.H. Kim, J.S. Kim, J.H. Jeong, J.K. Park, Y.J. Baik, K.S. Lee, B.K. Cheong, D. Kim, T.Y. Seong, and W.M. Kim, J. Nanosci. Nanotechnol. 12 (2012) 3665-3668.
19. J. Jia, A. Takasaki, N. Oka, and Y. Shigesato, J. Appl. Phys. 112 (2112) 013718.
20. D. Xu, Z. Deng, Y. Xu, J. Xiao, C. Liang, Z. Pei, and C. Sun, Phys. Lett. A 346 (2005) 148-152.21.
21. R. Das, K. Adhikary, and S. Ray, Appl. Surf. Sci. 253 (2007) 6068-6073.
22. J. Tauc, R. Grigorovichi, and A. Vancu, Phys. Stat. Sol. 15 (1966) 627-637.
23. D.H. Oh, Y.S. No, S.Y. Kim, W.J. Cho, J.Y. Kim, and T.W. Kim, J. Ceram. Proc. Res. 12 (2011) 488-491.